ISSN 1392 – 1215 ELECTRONICS AND ELECTRICAL ENGINEERING 2012. No. 6(122)
ELEKTRONIKA IR ELEKTROTECHNIKA

T 121 SIGNAL TECHNOLOGY
SIGNALŲ TECHNOLOGIJA

Feature Extraction and Reduction of Wavelet Transform Coefficients for EMG Pattern Classification

A. Phinyomark, A. Nuidod, P. Phukpattaranont, C. Limsakul
*Department of Electrical Engineering, Faculty of Engineering, Prince of Songkla University,
15 Kanjanavanich Road, Kho Hong, Hat Yai, Songkhla, 90112, Thailand,
e-mails: angkoon.p@hotmail.com, a.nuidod@gmail.com, pornchai.p@psu.ac.th, chusak.l@psu.ac.th*

crossref http://dx.doi.org/10.5755/j01.eee.122.6.1816

Introduction

Surface electromyography (sEMG) signals are among the most meaningful electro-physiological signals. However, the use of sEMG signals is challenging in both medical and engineering applications [1, 2] and in deploying sEMG signals as a diagnostic tool or a control signal, the feature extraction method is an important issue in achieving the optimal performance in classifying the sEMG pattern.

During the last two decades, many extraction techniques have been proposed in several domains [2], notably the time domain, the frequency domain and the time-frequency or time-scale domain. Among these techniques, features based on wavelet analysis are widely used as an efficient tool to extract useful information from the sEMG signal [3, 4].

Due to a complexity and non-stationarity of sEMG, a large number of studies have focused on the investigation and evaluation of the optimal features obtained from wavelet coefficients [4–15]. Many applications of pattern classification by wavelet analysis based on EMG feature extraction have been proposed, such as in sport science [5], determining muscle force and muscle fatigue [6–8], characterizing low-back pain [9], and identifying hand motions for the control of prostheses [4, 10–15].

Most studies to date have focused on applications classifying hand motions, and in the present study sEMG data were acquired from a volunteer performing six hand motions from two forearm muscles.

Discrete wavelet transform (DWT) is a time-scale approach that has been used successfully in many applications [16–18] and in the studies cited above, DWT has been successful in analysing non-stationary signals including sEMG signal. However, DWT yields a high-dimensional feature vector [10–12], that generally causes an increase in the learning parameters of a classifier [4]. Therefore, a method of reducing the dimensionality of the feature vector must be employed which preserves the classification accuracy [10]. Further, the classification performance resulting from using all the original wavelet coefficients is very poor judged both by computation cost and classification accuracy. For these reasons, the selection of the optimal dimensionality reduction method for the wavelet analysis is important before the feature vector is applied in the learning parameters of a classifier [11]. Commonly, dimensionality reduction methods can be implemented as methods of feature projection and feature selection [2, 11–13]. However, the feature projection approach shows superior results to the feature selection method [4]. Therefore, in this study only the projection method is considered.

The feature projection method attempts to determine the best combination of original wavelet coefficients and additionally, the features reduced are different from the original features. Commonly, the feature projection method is applied using principal component analysis (PCA) [19], an un-supervised linear transformation. However, different kinds of projection methods have been proposed such as the linear-nonlinear projection method consisting of a PCA and the self-organizing feature map (SOFM) [10], linear discriminant analysis (LDA) [11], and uncorrelated LDA [12].

Another approach that is frequently deployed for dimensionality reduction is extraction methods based on the time domain and the frequency domain [14, 15]. Many methods have been proposed during recent decades, for instance, energy, variance, mean absolute value (MAV), zero crossing (ZC), mean and median frequency, and auto-regressive coefficients. Due to the low complexity of extraction methods (e.g. MAV, ZC) compared with projection methods (e.g. PCA, SOFM), in this study we focus only on evaluating the performance of extraction methods based on the time domain and the frequency domain based on the reduction approach. Twenty-five state-of-the-art extraction methods are investigated.

However, all the studies mentioned above have deployed all the wavelet components or scales in the feature vector, whereas one of the main benefits of DWT is the generation of a useful subset of frequency components or scales from the signal of interest. Therefore, in this study we have investigated the usefulness of extracting features from individual wavelet components instead of extracting features from all the wavelet components [20–21]. As a result, beneficial resolution components were generated and selected from the sEMG signal [21–22], while unwanted components and noise were efficiently removed [20].

To achieve optimal performance in the wavelet analysis, a suitable wavelet function must be employed [23]. Most studies of sEMG analysis have concluded that the Daubechies (Db) wavelet family is the most suitable wavelet for sEMG signal analysis [6, 22, 23], and in this study, the Daubechies orthogonal wavelets, Db1-Db10, which are commonly used, were evaluated. To find an optimal combination between the components obtained from the wavelet (the wavelet basis function and the feature extraction method), a scatter graph of the features in space and a statistical measurement based on the ratio of the Euclidean distance to the standard deviation (RES index) [24] were used as the evaluation tools. An improvement of class separability in feature space of the EMG features is shown, which shoud lead to an increase in the classification accuracy of sEMG applications.

EMG signal acquisition and the experiment

The representative sEMG data were recorded when the volunteer performed six hand motions: wrist flexion (WF), wrist extension (WE), hand close (HC), hand open (HO), forearm pronation (FP) and forearm supination (FS). The data were recorded from two useful forearm muscles, the flexor carpi radialis muscle (FCR) and the extensor carpi radialis longus muscle (ECRL). Two bipolar-surface-electrodes (3M red dot 25 mm. foam solid gel) were placed directly on the right forearm. The electrodes were placed 20mm apart. In the experiment, ten datasets were collected for each motion. The sampling frequency was set at 1000 Hz using 16-bit data acquisition (BNC-2110, NI). A window size of 256 ms was used as a real-time constraint for prosthesis control where the response time should be less than 300 ms [4]. To avoid noise and the amplifying amplitude of the sEMG, a band-pass filter of 10-500 Hz bandwidth, with a CMRR of 100 dB, and an amplifier with 60 dB gain were implemented. All the calculations based on the data derived from the experiments in this study were computed using the MATLAB software.

The wavelet transform and its features

The wavelet transform method can be divided into two types: discrete (DWT) and continuous (CWT). DWT was selected in this study because of its concentration on real-time applications. Briefly, the DWT technique iteratively transforms the signal of interest into multi-resolution subsets of coefficients, and then the original sEMG (S) is passed through high-pass and low-pass filters, the coefficients of the filters depending on the wavelet function type, to yield both a detailed coefficient subset (cD1) and an approximation coefficient subset (cA1) at the first level. To achieve a multi-resolution analysis, repetitious transformation is performed. This process is duplicated until the desired final level is yielded.

Different levels of wavelet decomposition (*n*) were also evaluated in the experiments with the maximum level limited to 8 and the fixed sample length at 256 samples. As an illustration, if the decomposition level was set at 4, DWT generates respectively the coefficient subsets at the fourth level approximation (cA4) and the first to the fourth level details (cD1, cD2, cD3 and cD4). After that each wavelet coefficient subset can be reconstructed to estimate an effective sEMG component by using the inverse discrete wavelet transform (IDWT) which is computed by using the coefficients of all the wavelet components at the final decomposition level. The reconstructed sEMG signal can then be computed from cA4 and cD1-cD4.

To investigate the usefulness of extracting features from individual wavelet components instead of extracting them from all the components, the reconstructed sEMG can be defined by the inversion of the subset dependence. For instance, in order to obtain the estimated sEMG signal from the approximation coefficient subset, the reconstructed sEMG signal (A4) is computed by using IDWT with the fourth-level approximation coefficients (cA4). The wavelet coefficient subsets (cD1-cDn, cAn) and the reconstructed sEMG signals (D1-Dn, An) can then be used as the features of the six motions of the two muscles.

In this study, the most widely used and most successful 25 features based on the time domain and the frequency domain were evaluated. The mathematical definition of all the features is shown in Table 1. The procedure adopted in the study is shown in Fig. 1. Comparisons of class separability for each extraction type were conducted to establish a suitable sEMG subset based on the RES index. More details about the RES index can be found in [24].

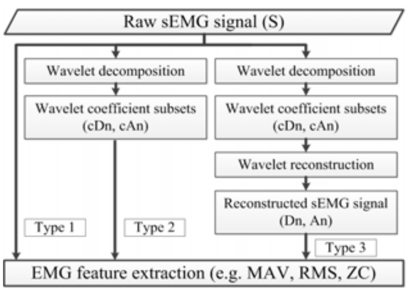

Fig. 1. Procedure for the extraction of sEMG features from the raw wavelet coefficients and the reconstructed sEMG signals.

Experimental results and discussion

The results relating to the 4 issues mentioned above (wavelet components, wavelet function, decomposition level, and feature extraction method) are reported on and discussed below. The optimal wavelet decomposition level is discussed first because the results are not dependent on the type of wavelet function or the feature extraction method. The results showed that the best decomposition level is 4; hence, only the results obtained from the fourth-

Table 1. Mathematical definitions of 25 sEMG feature extraction methods. Let x_n represents the n^{th} sample of the sEMG signal (S) or the wavelet coefficient subsets (cDn, cAn) or the reconstructed sEMG signals (Dn, An) in a window segment. N denotes the length of the sEMG signal. w_n is the continuous weighting window function. *threshold* is used to avoid low-voltage fluctuations or background noises. P_j is the sEMG power spectrum at frequency bin j. f_j is the frequency of the sEMG power spectrum at frequency bin j. M is the length of the frequency bin. f_0 is a feature value of the PKF. nl is the integral limit (nl = 20). P_0 is near to the maximum value of the sEMG power spectrum. P is the whole energy of the sEMG power spectrum in a range of 10 and 500 Hz

Feature extraction	Mathematical definition
Integrated EMG (IEMG)	$\mathrm{IEMG} = \sum_{n=1}^{N} \lvert x_n \rvert$
Mean absolute value (MAV)	$\mathrm{MAV} = \frac{1}{N}\sum_{n=1}^{N} \lvert x_n \rvert$
Modified Mean Absolute Value (MMAV)	$\mathrm{MMAV} = \frac{1}{N}\sum_{n=1}^{N} w_n \lvert x_n \rvert$; $w_n = \begin{cases} 1, & if\ 0.25N \le n \le 0.75N \\ 0.5, & \text{otherwise} \end{cases}$
Simple Square Integral (SSI)	$\mathrm{SSI} = \sum_{n=1}^{N} \lvert x_n \rvert^2$
Variance of EMG (VAR)	$\mathrm{VAR} = \frac{1}{N-1}\sum_{n=1}^{N} x_n^2$
Root Mean Square (RMS)	$\mathrm{RMS} = \sqrt{\frac{1}{N}\sum_{n=1}^{N} x_n^2}$
v-Order 2 and 3 (V2, V3)	$\mathrm{V2} = \left(\frac{1}{N}\sum_{i=1}^{N} x_i^2\right)^{\frac{1}{2}}; \mathrm{V3} = \left(\frac{1}{N}\sum_{i=1}^{N} \lvert x \rvert_i^3\right)^{\frac{1}{3}}$
Log detector (LOG)	$\mathrm{LOG} = e^{\frac{1}{N}\sum_{n=1}^{N}\log(\lvert x_n \rvert)}$
Waveform length (WL)	$\mathrm{WL} = \sum_{n=1}^{N-1} \lvert x_{n+1} - x_n \rvert$
Average amplitude change (AAC)	$\mathrm{AAC} = \frac{1}{N}\sum_{n=1}^{N-1} \lvert x_{n+1} - x_n \rvert$
Difference absolute standard deviation value (DASDV)	$\mathrm{DASDV} = \sqrt{\frac{1}{N-1}\sum_{n=1}^{N-1}(x_{n+1} - x_n)^2}$
Maximum Fractal Length (MFL)	$\mathrm{MFL} = \log_{10}\left(\sqrt{\sum_{n=1}^{N-1}(x_n - x_{n+1})^2}\right)$
Myopulse percentage rate (MYOP)	$\mathrm{MYOP} = \frac{1}{N}\sum_{i=1}^{N}[f(x_i)]$; $f(x) = \begin{cases} 1, & if\ x \ge threshold \\ 0, & \text{otherwise} \end{cases}$
Zero crossing (ZC)	$\mathrm{ZC} = \sum_{n=1}^{N-1}[\mathrm{sgn}(x_n \times x_{n+1}) \cap \lvert x_n - x_{n+1} \rvert \ge 0]$; $\mathrm{sgn}(x) = \begin{cases} 1, & if\ x \ge 0 \\ 0, & \text{otherwise} \end{cases}$
Willison amplitude (WAMP)	$\mathrm{WAMP} = \sum_{n=1}^{N-1} f(\lvert x_n - x_{n+1} \rvert)$; $f(x) = \begin{cases} 1, & if\ x \ge threshold \\ 0, & \text{otherwise} \end{cases}$
Mean power (MNP)	$\mathrm{MNP} = \sum_{j=1}^{M} P_j \Big/ M$
Total power (TTP)	$\mathrm{TTP} = \sum_{j=1}^{M} P_j$
Median Frequency (MDF)	$\sum_{j=1}^{\mathrm{MDF}} P_j = \sum_{j=\mathrm{MDF}}^{M} P_j = \frac{1}{2}\sum_{j=1}^{M} P_j$
Mean Frequency (MNF)	$\mathrm{MNF} = \sum_{j=1}^{M} f_j P_j \Big/ \sum_{j=1}^{M} P_j$
Peak frequency (PKF)	$\mathrm{PKF} = \max(P_j),\quad j = 1,...,M$
Frequency ratio (FR)	$\mathrm{FR} = \sum_{j=LLC}^{ULC} P_j \Big/ \sum_{j=LHC}^{UHC} P_j$
Power spectrum ratio (PSR)	$\mathrm{PSR} = \frac{P_0}{P} = \sum_{j=f_0-nl}^{f_0+nl} P_j \Big/ \sum_{j=-\infty}^{\infty} P_j$
The 1st, 2nd, and 3rd spectral moments (SM1, SM2, SM3)	$\mathrm{SM1} = \sum_{j=1}^{M} P_j f_j$; $\mathrm{SM2} = \sum_{j=1}^{M} P_j f_j^2$; $\mathrm{SM3} = \sum_{j=1}^{M} P_j f_j^3$

level are presented. In addition, similar results have been reported in a number of previous studies [e.g. 6, 12, 14]. However, the most suitable level for the analysis of sEMG is the fourth level. The other three issues are discussed in the remainder of this section.

Fig. 2 shows examples of characteristic signals computed from the three approaches described in Fig. 1 based on the Db7 wavelet from the HC motion and the FCR muscle. The signals obtained from the raw sEMG signal (Type I), the wavelet coefficient subsets at different multi-resolution levels (Type II), and the reconstructed sEMG signals at different multi-resolution levels (Type III) are presented in Fig. 2. In most types of natural signals the low-frequency components (cA4 and A4) are generally the most important componenents and can be regarded as the characteristics of the signal, whereas the high-frequency components (cD1-cD4 and D1-D4) can be assumed to be noise. In this study, the low-frequency components (cA4 and A4) of the sEMG contain indirect correspondence and also contain an irrelevant low-resolution background, whereas, the signals at the first and the second decomposition levels (cD1 and cD2), and the first and the second reconstruction levels (D1 and D2) are similar to the original sEMG signal (S). Therefore the signals cD1, cD2, D1 and D2 were adopted for analysis as being the most useful sEMG components.

In evaluating the performance of sEMG feature extraction methods, class separability is a major criterion. Good quality class separability means that the result in terms of classification accuracy will be as high as possible with the maximum separation between classes and a minimum of variation in the subject experiment. In this study, two statistical measurement methods, a scatter graph and the RES index were used as the evaluation criteria to confirm the observations from Fig. 2. The selection of sEMG features was based on a statistical index because evaluation results based on a classifier are dependent on the type of classifier [15].

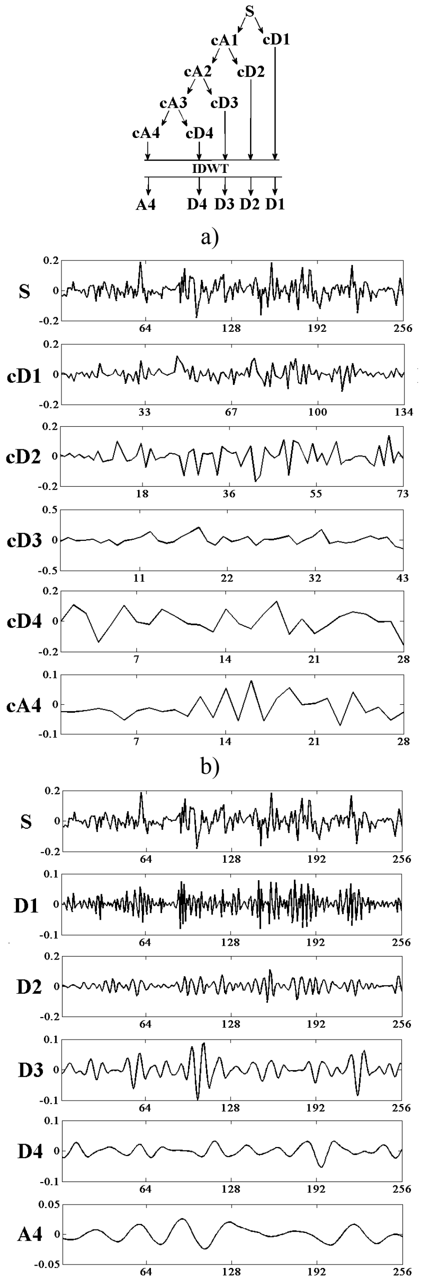

Fig. 2. (a) DWT decomposition tree from decomposition level 4 and the inverse transform for each subset. (b, c) Examples of the sEMG signal using wavelet multi-resolution analysis with Db7 wavelet and 4-level decomposition and reconstruction of the raw sEMG signal (S), reconstructed sEMG signals (D1-D4, A4), and wavelet coefficient subsets (cD1-cD4, cA4) of HC motion from the FCR muscle.

Fig. 3 is an example of a scatter graphs of the MAV features extracted from the two channels and six upper-limb motions illustrating the distance between the two scatter groups and the variation of features in the same group. The figure shows the scatter plots of the MAV extracted from the raw sEMG signal (S) and the low-level wavelet coefficient subset and the reconstructed sEMG signal (cD1 and D2) which indicate a clear separation in data points from each motion with only a small degree of variation within the same group. This indicates that the EMG feature vector obtained from these signals is able to yield good classification from the classifier. On the other hand, the scatter plot of MAV computed from the high-level reconstructed sEMG signal (A4) (and also the high-level wavelet coefficient subset, cA4) has, in comparison, poor class separability. However, the classification performance between the raw sEMG signal, the low-level wavelet reconstructed sEMG signals, and the low-level wavelet coefficient subsets are difficult to observe from a scatter graph. Hence, to confirm the class separability performance, the RES index is used to indicate the quality of separation. It should be noted that the values of the RES index for S, cD1, D2 and A, in Fig. 3, are 8.93, 10.60, 11.11 and 5.57, respectively.

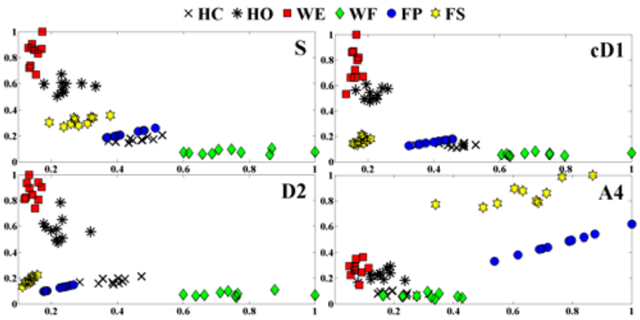

Fig. 3. Scatter plots of the MAV feature calculated from the raw sEMG signal (S), the wavelet's detail coefficient subset at the first level (cD1), the reconstructed sEMG signal from the cD2 (D2), and the reconstructed sEMG signal from cA4 (A4) with six hand motions and two channels (*FCR muscle*–X axis, *ECRL* muscle–Y axis)

Table 2. The optimal wavelet component and wavelet function for the 25 sEMG features considered in this study with their RES indices

Feature extraction	Optimal wavelet component	Optimal WF	RES index
ZC			12.52
WAMP			12.22
MAV, IEMG			11.11
VAR, SSI, TTP, MNP	D2	Db7	10.83
MMAV			10.69
SM1			10.45
LOG			9.53
RMS, V2			11.06
V3	cD1	Db10	10.27
SM2			10.23
SM3			9.83
MYOP	D1	Db5	12.95
MFL		Db8	9.86
WL, AAC			11.69
DASDV			11.15
MNF	Raw	-	5.48
MDF			5.38
PSR			4.99
FR			3.46

Table 2 shows the RES index for all features with the optimal wavelet function and wavelet component type.

The experimental results show that the suitability of wavelet components and wavelet functions depend on the type of feature (i.e. they are feature dependent). The results can be divided into four main groups:

1). The first group contains most of the features based on the time domain and some from the frequency domain that are calculated based on amplitude and energy properties. In this group, the RES indices calculated from the second-level reconstructed sEMG signal (D2) with Db7 showed better class separability in feature space compared to the RES indices calculated from the original sEMG signal (S). The features in this group are eight time-domain features: IEMG, MAV, MMAV, SSI, VAR, LOG, ZC and WAMP and three features based on the frequency-domain: TTP, MNP and SM1. However, the frequency-domain features determine the energy property in the same way as do features in the time domain. The best feature in this group is ZC, followed closely by WAMP, MAV and IEMG;

2). The second group contains higher-order time and frequency domain features including RMS, V2, V3, SM2 and SM3. The RES indices in this group register an improvement in class separability in feature space if calculated from the first-level wavelet coefficient subset (cD1) with Db10. The best feature in this group is RMS, although its performance is no better than the best features in the first group;

3). The third group contains only 2 features, MYOP and MFL. These features perform better when calculating features from the first-level reconstructed sEMG signal (D1) with the Db8 and the Db5 wavelets. The RES index obtained from MYOP has the highest value (12.95);

4). The last group contains 3 time-domain features, WL, AAC and DASDV, based on complexity and 4 popular frequency-domain features, MDF, MNF, FR and PSR. The RES indices of features in the last group were different from those of other groups. The results show that the use of the raw sEMG signal (S) for this group was superior to using wavelet analysis.

As mentioned in the introduction, the main benefit of DWT is that it generates a useful subset of frequency components, although most earlier studies have used all of the frequency components in the feature vector. This study used only the most effective components instead of using all the components available. These more useful resolution components from sEMG signal were generated and selected during the experiment.

In summary, the reconstructed sEMG signals from the first level and the second level of the wavelet's detail coefficients are most suitable for the extraction of sEMG features. On the other hand, other wavelet components contain noise and unwanted sEMG parts, and extraction of sEMG features from those components does not improve classification ability.

In future studies, we recommend extracting sEMG features from the reconstructed sEMG signals from the first and second levels (D1 and D2) instead of using all the wavelet components. This would not only improve the accuracy of the sEMG pattern classification but also decrease the computational time and complexity due to the reduction in sub-signals. Moreover, in order to confirm the classification performance, misclassification rates resulting from the use of a classifier should be measured in future studies.

Because wavelet transforms are capable of multi-resolution, the frequency band that signals from each motion generate has been discussed. The results of this study based on decomposition down to 8 levels by using db7 prove that sEMG signal from different motions exhibit differences in their main signal energy corresponding to those of the muscles whose motions are measured, for instance, WF, WE and HC co-vary with levels D1, D2 and D3, HO with levels D2 and A8, FP with levels D6, D8, and A8, and FS with level A8. These correspondences could be used to develop a system for sEMG signal interpretation by using the signal energy distribution of the wavelet coefficients to enhance signal recognition.

Conclusions

The usefulness of successful sEMG features extracted from multiple-level decompositions of sEMG based on DWT has been investigated in this paper. Some useful sEMG features are recommended, for instance, a feature vector extracted by using the ZC, WAMP and MAV features of the second-level reconstructed sEMG signal (D2) with the Db7 wavelet, and the MYOP feature of the first-level reconstructed sEMG signal (D1) with the Db8 wavelet. Their use ensures that the resulting classification accuracy will be as high as possible and will also be better than signal extraction from the original sEMG signal. The results of the experiment reported in this paper can be used in a wide class of clinical and engineering applications.

Acknowledgements

This work was supported by the Thailand Research Fund through the Royal Golden Jubilee Ph. D. Program (Grant No. PHD/0110/2550).

References

1. **Canal M. R.** Comparison of Wavelet and Short Time Fourier Transform Methods in the Analysis of EMG Signals // Journal of Medical Systems. – Springer, 2010. – Vol. 34(1). – P. 91–94.
2. **Oskoei M. A., Hu H.** Myoelectric Control Systems–A Survey // Biomedical Signal Processing and Control. – Elsevier, 2007. – Vol. 2(4). – P. 275–294.
3. **Pauk J.** Different Techniques for EMG Signal Processing // Journal of Vibroengineering. – Vibroengineering, 2008. – Vol. 10(4). – P. 571–576.
4. **Englehart K., Hudgins B., Parker P. A.** A Wavelet–Based Continuous Classification Scheme for Multifunction Myoelectric Control // IEEE Transactions on Biomedical Engineering. – IEEE, 2001. – Vol. 48(3). – P. 302–311.
5. **Neto O. P., Marzullo A. C. D.** Wavelet Transform Analysis of Electromyography Kung Fu Strikes Data // Journal of Sports Science and Medicine. – Asist Group, 2009. – Vol. 8(CSSI 3). – P. 25–28.
6. **Hussain M. S., Reaz M. B. I., Mohd–Yasin F., Ibrahimy M. I.** Electromyography Signal Analysis Using Wavelet Transform and Higher Order Statistics to Determine Muscle Contraction // Expert Systems. – John Wiley & Sons, 2009. – Vol. 26(1). – P. 35–48.
7. **Delis A. L., Carvalho J. L. A., Rocha A. F. d., Ferreira R. U., Rodrigues S. S., Borges G. A.** Estimation of the Knee Joint Angle from Surface Electromyographic Signals for

Active Control of Leg Prostheses // Physiological Measurement. – IOP, 2009. – Vol. 30(9). – P. 931–946.
8. **Daniuseviciute L., Pukenas K., Brazaitis M., Skurvydas A., Sipaviciene S., Ramanauskiene I., Linonis V.** Wavelet–Based Entropy Analysis of Electromyography during 100 Jump // Electronics and Electrical Engineering. – Kaunas: Technologija, 2010. – No. 8(104). – P. 93–96.
9. **Kumar S., Prasad N.** Torso Muscle EMG Profile Differences between Patients of Back Pain and Control // Clinical Biomechanics. – Elsevier, 2010. – Vol. 25(2). – P. 103–109.
10. **Chu J. U., Moon I., Mun M. S.** A Real–Time EMG Pattern Recognition System Based on Linear–Nonlinear Feature Projection for a Multifunction Myoelectric Hand // IEEE Transactions on Biomedical Engineering. – IEEE, 2006. – Vol. 53(11). – P. 2232–2239.
11. **Chu J. U., Moon I., Lee Y. J., Kim S. K., Mun M. S.** A Supervised Feature–Projection–Based Real–Time EMG Pattern Recognition for Multifunction Myoelectric Hand Control // IEEE/ASME Transactions on Mechatromics. – IEEE, 2007. – Vol. 12(3). – P. 282–290.
12. **Wang G., Wang Z., Chen W., Zhuang J.** Classification of Surface EMG Signals Using Optimal Wavelet Packet Method Based on Davies–Bouldin Criterion // Medical and Biological Engineering and Computing. – Springer, 2006. – Vol. 44(10). – P. 865–872.
13. **Chan A. D. C., Green G. C.** Myoelectric Control Development Toolbox // Proceedings of 30th Conference of the Canadian Medical & Biological Engineering Society. – 2007. – Vol. 1. – P. M0100-1–M0100-4.
14. **Hu X., Wang Z., Ren X.** Classification of Surface EMG Signal Using Relative Wavelet Packet Energy // Computer Methods and Programs in Biomedicine. – Elsevier, 2005. – Vol. 79(3). – P. 189–195.
15. **Boostani R., Moradi M. H.** Evaluation of the Forearm EMG Signal Features for the Control of a Prosthetic Hand // Physiological Measurement. – IOP, 2003. – Vol. 24(2). – P. 309–319.
16. **Gokmen G.** Wavelet Based Reference Current Calculation Method for Active Compensation Systems // Electronics and Electrical Engineering. – Kaunas: Technologija, 2011. – No. 2(108). – P. 61–66.
17. **Popov A., Kanaykin A., Zhukov M., Panichev O., Bodilovsky O.,** Adapted Mother Wavelets for Identification of Epileptiform Complexes in Electroencephalograms // Electronics and Electrical Engineering. – Kaunas: Technologija, 2010. – No. 8(104). – P. 89–92.
18. **Georgieva V. M.** An Approach for Computed Tomography Images Enhancement // Electronics and Electrical Engineering. – Kaunas: Technologija, 2010. – No. 2(98). – P. 71–74.
19. **Englehart K., Hudgins B., Parker P. A., Stevenson M.** Classification of the Myoelectric Signal Using Time–Frequency Based Representations // Medical Engineering & Physics. – Elsevier, 1999. – Vol. 21(6–7). – P. 431–438.
20. **Yang G. Y., Luo Z. Z.** Surface Electromyography Disposal Based on the Method of Wavelet De–Noising and Power Spectrum // Proceedings of International Conference on Intelligent Mechatronics and Automation. – IEEE, 2004. – Vol. 1. – P. 896–900.
21. **Buranachai C., Thavarungkul P., Kanatharana P., Meglinski I. V.** Application of Wavelet Analysis in Optical Coherence Tomography for Obscured Pattern Recognition // Laser Physics Letters. – John Wiley & Sons, 2009. – Vol. 6(12). – P. 892–895.
22. **Mahaphonchaikul K., Sueaseenak D., Pintavirooj C., Sangworasil M., Tungjitkusolmun S.** EMG Signal Feature Extraction Based on Wavelet Transform // Proceedings of the 7th International Conference on Electrical Engineering/ Electronics, Computer, Telecommunications. – IEEE, 2010. – Vol. 1. – P. 356–360.
23. **Phinyomark A., Limsakul C., Phukpattaranont P.** Optimal Wavelet Functions in Wavelet Denoising for Multifunction Myoelectric Control // ECTI Transactions on Electrical Eng., Electronics, and Communications. – ECTI, 2010. – Vol. 8(1). – P. 43–52.
24. **Phinyomark A., Hirunviriya S., Limsakul C., Phukpattaranont P.** Evaluation of EMG Feature Extraction for Hand Movement Recognition Based on Euclidean Distance and Standard Deviation // Proceedings of the 7th International Conference on Electrical Engineering/ Electronics, Computer, Telecommunications and Information Technology. – IEEE, 2010. – Vol. 1. – P. 856–860.

Received 2011 09 11
Accepted after revision 2012 01 02

A. Phinyomark, A. Nuidod, P. Phukpattaranont, C. Limsakul. Feature Extraction and Reduction of Wavelet Transform Coefficients for EMG Pattern Classification // Electronics and Electrical Engineering. – Kaunas: Technologija, 2012. – No. 6(122). – P. 27–32.

Recently, wavelet analysis has proved to be one of the most powerful signal processing tools for the analysis of surface electromyography (sEMG) signals. It has been widely used in sEMG pattern classification for both clinical and engineering applications. This study investigated the usefulness of extracting sEMG features from multiple-level wavelet decomposition and reconstruction. A suitable wavelet based function was used to yield useful resolution components from the sEMG signal. The optimal sEMG resolution component was selected and then its reconstruction carried out. Throughout this process, noise and unwanted sEMG components were removed. Effective sEMG components were extracted with twenty-five state-of-the-art features in both the time domain and the frequency domain. Two criteria were deployed in the evaluation, scatter graphs and a class separation index. The experimental results show that most sEMG features extracted from the reconstructed sEMG signal of the first and second-level wavelet detail coefficients yield improved class separability in feature space. Some features extracted from the sub-signals are recommended such as the myopulse percentage rate, zero crossing, Willison amplitude and the mean absolute value. The proposed method will ensure that the classification accuracy will be as high as possible while the computational time will be as low as possible. Ill. 3, bibl. 24, tabl. 2 (in English; abstracts in English and Lithuanian).

A. Phinyomark, A. Nuidod, P. Phukpattaranont, C. Limsakul. Požymių išskyrimas ir vilnelių transformacijos koeficientų sumažinimas elektromiografijos atvaizdams klasifikuoti // Elektronika ir elektrotechnika. – Kaunas: Technologija, 2012. – Nr. 6(122). – P. 27–32.

Vilnelių transformacija yra vienas iš geriausių signalų apdorojimo įrankių atliekant paviršinės elektromiografijos (pEMG) signalų analizę. Ji plačiai naudojama klasifikuojant pEMG atvaizdus tiek klinikinėse, tiek inžinerinėse taikomosiose programose. Panaudota tinkama vilnelių funkcija siekiant gauti tinkamos rezoliucijos komponentus iš pEMG signalo. Buvo parinktas optimalus pEMG rezoliucijos komponentas ir atlikta jos rekonstrukcija. Šio proceso metu buvo pašalintas triukšmas ir nepageidaujami pEMG komponentai. Eksperimentiniai rezultatai parodė, kad dauguma pEMG bruožų, išskirtų iš rekonstruoto pEMG signalo, padeda geriau atskirti klases bruožų erdvėje. Pasiūlytas metodas užtikrina kiek įmanoma didesnį klasifikacijos tikslumą ir mažesnę skaičiavimo trukmę. Il. 3, bibl. 24, lent. 2 (anglų kalba; santraukos anglų ir lietuvių k.).